Humidity Sensor Based on Etched Optical Fibers Coated With Graphene Composite

F. Ostovari (ostovari@yazd.ac.ir)
Yazd University
E. Owji
Yazd University
H. Mokhtari Iran
Yazd University

Research Article

Keywords: Graphene oxide, Optical fiber, Relative humidity, Humidity sensor, Silica gel, Optical sensor

Posted Date: May 28th, 2021

DOI: https://doi.org/10.21203/rs.3.rs-558959/v1

Abstract

In this research, optical humidity sensors based on etched-optical fibers coated with graphene Oxide (GO), silica gel (Sg) and a silica gel modified with GO (GSg) was studied. Their humidity sensing behavior was investigated by variation of relative differentiation of attenuation (RDA) in the presence of relative humidity (RH). As the results showed, etched fibers coated with Sg and GSg are highly capable of humidity sensing. However, a Sg- coated sample is not useful as humidity sensor related to sample coated by GSg because its RDA lacks a one-to-one correspondence with RH. As it was also found, the sensitivity of a GSg-coated sample is higher when the RH is below 40% and its repeatability is considerable.

Introduction

Optical fibers have a vital role in telecommunications and serve as a substitute for copper cables. This is owing to their great advantages such as high speed, insensitive to electromagnetic interference, being anti-explosion, the small size of cables, durability, and chemical inertness (1). In recent years, optical fibers have been commonly used as sensors, and they have developed rapidly for biomedical and home security purposes (2). The function of these sensors is very dependent on the changes in the refractive index. In this regard, one may refer to LPG gas sensors (3) and U-shaped bending-induced interference sensors (4). Optical fiber sensors can be used to measure different physical properties, such as RI, strain (5), temperature (6, 7) and humidity (6–12). So far, various types of humidity-sensing fibers, such as side-polished fibers, long-period fiber gratings (LPFG) and hollow-core fiber sensors, have been reported (13–16). Despite their advantages, the methods of fabricating these sensors are very complicated.

Moreover, nanostructures such as monolayers as well as a few graphene (G) and graphene oxide (GO) compounds have proved to be greatly potential for high-sensitivity applications. Their applicability in this case is due to their high surface- to- volume ratio and intrinsic properties (12, 16–28).

Graphene has hydrophobic properties, but GO is hydrophilic because of its oxygen-containing functional groups, which makes it possible to adsorb polar molecules such as water molecules (13, 29, 30).

High sensitivity, extensive range, fast response and short recovery time are the important industry requirements to meet. To achieve these features, it is necessary to coat optical fibers with other materials and make certain physical changes on the structure of those fibers.

In this study, some optical sensors are developed individually based on GO and silica gel (Sg) as a common humidity absorbent. Also, for the first time, a combination of GO and Sg (GSg) is used to improve the relative humidity (RH) sensing of etched optical fibers. These products have the benefits of non-complicated fabrication and short processing time.

Materials And Methods

At first, 2D layers of GO, Sg and GSg were synthesized and qualified. To achieve a desirable evanescence field by reducing the diameter of the fibers, a part of the single-mode fibers (SMFs) was corroded with hydrofluoric acid (HF) for 60 minutes. Then, the synthesized materials were coated on the surface of the etched fibers by the dip coating method. At the end, the optical loss test set (OLTS) as a tool of analysis, the optical power source (OPS) and the optical power meter (OPM) were used to investigate the optical humidity sensing of the fibers.

A. Synthesis

A GO layer was synthesized by the liquid-phase exfoliation of graphite oxide. After the synthesis of graphite oxide powder by Hummer's method (31–34), 5 mgr of the powder was added to10 cc of distilled water, and the solution was sonicated to separate the individual graphite oxide layers. A transparent liquid was obtained with sediments that contained a few monolayers of GO. The liquid was centrifuged at 4000 rpm for three hours. The quality of the GO layers was investigated by SEM (Scanning Electron Microscopy), TEM (Transmission Electron Microscopy), Raman, FTIR (Fourier-transform infrared spectroscopy) and XRD (X-ray Diffraction).

The TEM and AFM images show the microstructure of the synthesized GO (Fig. 1A and 1B). The FTIR spectrum shows the presence of C-O, C = O and C–H bands at 1020, 1624 and 2,923 cm^{-1} respectively (Fig. 1C). The spread peak in the region of 3430 is related to the tensile vibration of phenol(C-OH) groups (35, 36).

The Raman spectrum of the GO layer exhibits two important peaks called D and G bands around 1197 and 1634 cm^{-1} respectively (37, 38). The G band shows the presence of sp^2 carbon-type structures within the sample, and the D band is associated with defects in the hexagonal structure of graphite (Fig. 1D).

The UV/Visible absorption of the GO solutions was measured and plotted in Fig. 1E. As the figure shows, the transparency of GO is obvious, and wavelength peak of ~ 310 nm corresponds to the n – n∗ transitions of carbonyl group (39, 40).

The X-ray diffraction (XRD) of the GO sheets illustrated peaks at 2θ = 10° (d001 = 0.83 nm), 2θ = 20° (d002 = 0 .48 nm), 2θ = 26° (d002 = 0 34 nm) and 2θ = 55° (d004 = 0 .17 nm). The peaks at 2θ = 26°and 55° were characteristic of graphite and its chemical oxidation (Fig. 1F). Basically, as the inter- planar distance increases, the other peaks appear (37, 41).

Sg was produced by the heating of silicic acid (pH ~ 3) at70^{o}C for two hours to form a gel. Figure 2A and Fig. 2B present the TEM image and the energy-dispersive X-ray spectroscopy (EDX) of Sg. As the TEM image shows, no SiO_2 nano-particles are formed in the Sg structure. In addition, the identification of Si and O in the EDX analysis implies the purity of Sg.

A GSg was prepared by adding 20 cc of a transparent solution containing GO to 100 cc of silicic acid. Then, the mixture was heated at 70^{o}C to form the gel. Figure 2C illustrates the SEM image of the GSg that

is coated on silicon oxide wafer.

B. The Setup of the humidity sensing experiment

In order to make the fiber sensor, 3 cm of the protective layer of a fiber was stripped. Then, it was wiped up with alcohol and corroded with HF for about 60 minutes to achieve a desirable evanescence field. The achieved diameter of the etched-fiber was 32.5 µm. The SEM image of this etched-fiber is presented in Fig. 3A. Basically, etching a fiber leads to the reduction of its clad and the creation of an evanescence field. After etching, the clad mode is significantly increased, and the wavelength of incident light shifts to a longer wavelength (i.e. it becomes red-shifted) (18, 42). Figure 3B shows the etched SMF coated with GSg.

The produced sensor was placed in a humidity control box. An OPS and an OPM (OLTS) were attached to the ends of the fiber. Figure 3C shows the employed temperature controller (set on 25°C), standard humidity sensor (to compare to our humidity sensor) and humidifier (to increase the relative humidity of the environment within the range of 20–90% RH).

Results And Discussion

The relative differentiation of attenuation (RDA) as a function of RH is illustrated in Fig. 4. The values belong to GO, Sg and GSg at both standard telecommunication wavelengths of 1310 nm and 1550 nm. All the measurements were performed by OLTS at a room temperature.

At the first look, it seems that the etched fibers coated with Sg are good humidity sensors due to the good absorption and release of humidity by Sg. However, as in the figure, the fibers have a high RDA value which has no one-to-one correspondence with RH. This makes the fibers unusable for humidity sensing. Moreover, the RDAs versus RH are the same for both 1310-nm and 1550-nm wavelengths.

Despite the well-known rapid and excellent sensing properties of GO (30), the etched fibers coated with it have a zero and low RDA value below and above 40% RH respectively. Also, the difference between the curves are obvious for both 1310-nm and 1550-nm wavelengths. The main advantage of the GO-coated fibers over the Sg-coated ones is the one-to-one correspondence of their RDA with RH (Fig. 4).

The sensing mechanism for the etched fibers coated with GO is based on their refractive index variations. As the humidity in the environment increases, more water molecules are adsorbed to the GO. This changes the gap between the GO and the fiber refractive indices. When water molecules reach near the surface of GO, they become ionized ($2H2O \Leftrightarrow H3O+ + OH-$) and make bonds with phenol ($C-OH$) or carbonyl ($C=O$) in the GO groups (18, 43). The adsorption of water molecules onto the GO leads to a change in its electrical energy gap and, thus, a change in its refractive index.

The etched fibers coated with GSg have a non-zero incremental behavior, and their RDA has a one-to-one correspondence with RH. These fibers are, therefore, more reasonable than the others to be used as

humidity sensors. Their RDA intensity is also higher at 1550 nm, which is because of the existence of GO in their coated layer.

Since repeatability is an important quality of sensors, the measurement of RDA versus RH was instantly repeated for the etched fibers coated with GSg, and the re-test curve was obtained. Figure 5A and Fig. 5C show the good repeatability of this humidity sensor. To calculate the RH from attenuation, the reverse curves were fitted by MATLAB (Fig. 5B and Fig. 5D).

Another key parameter of sensors is sensitivity. It has been defined as the ratio of the output signal to the initial signal of a humidity sensor (44). As shown in Fig. 6a, the sensitivity of GSg at the 1550-nm wavelength was higher than that at 1310 nm. Also, GSg had higher sensitivity at a low RH index (less than 50%). So, it can be more useful in this humidity range. The variance of each test from the average value is plotted in Fig. 6b. As it can be seen, the variance for the investigated sensor was small at RH values less than 50%. In addition, the variance was smaller at the 1550-nm wavelength than at 1310 nm. These findings prove the higher accuracy of the GSg- coated sensor for low-humidity conditions (under 50%) and at the 1550-nm wavelength.

This research was conducted to evaluate the ability of etched SMFs coated with GO, Sg and GSg and used as a humidity sensor. For this purpose, RDA was analyzed in the presence of RH and at both standard wavelengths of telecommunication, namely 1310 nm and 1550 nm. As the results showed, etched SMFs coated with Sg are not useful for humidity sensing. It is due to lack of a one-to-one correspondence of their RDA versus RH although the RDA is high. Also, GO-based etched fibers have a low RDA value. Of the three samples, etched SMFs coated with GSg have proved to be the best humidity sensors. Their RDA is relatively high and has a one-to-one correspondence with RH. Besides, their repeatability and sensitivity are reasonable, and their low variance is suggestive of their accuracy. The proposed GSg-based etched SMFs have high, rapid, repeatable and accurate responses at RH indices below 40%. So, they can be used as low-humidity sensors.

Declarations

Acknowledgments

This research was supported by Shahid Ghandi Corporation Complex for technical measurement tools.

Data Availability

The data that supports the findings of this study are available within the article.

References

1. J. L. Santos, F. Farahi, “Fiber-Optic Sensors,” in *Hand book of optical Sensors*, 1st ed., CRC Press, 2018, sec III, pp. 257-587.

2. A. Cusano, M. Consales, A. Crescitelli, A. Ricciardi, Lab-on-fiber technology, Springer Series in Surface Sciences; *Springer International Publishing: Cham*, Vol. 56, 2015, ISBN 978-3-319-06997-5.
3. C. W. Wu, C. C. Wu, C. C. Chiang, "A ZnO nanoparticle-coated long period fiber grating as a carbon dioxide gas sensor," *Inventions*, vol. 1, pp. 21, 2016.
4. Y. L. Fang, C. T. Wang, C.C. Chiang, "A small U-shaped bending- induced interference optical fiber sensor for the measurement of glucose solutions," *Sensors*, vol. 16, pp. 1460, 2016**.**
5. M. Pisco, F.A. Bruno, G. Danilo, L. Nardone, G. Gruca, N. Rijnveld, F.Bianco, A. Cutolo, A. Cusano, "Seismic sensors detected the Norcia earthquake," *Scientific Reports*, vol. 8, pp. 6680, 2018.
6. G. Woyessa, A. Fasano, C. Markos, H.K. Rasmussen, O. Bang, "Low loss polycarbonate polymer optical fiber for high temperature FBG humidity sensing," *IEEE Photonics Technol. Lett.*, vol. 29, pp. 575–578, 2017.
7. G. Woyessa, K. Nielsen, A. Stefani, C. Markos, O. Bang, "Temperature insensitive hysteresis free highly sensitive polymer optical fiber Bragg grating humidity sensor," *Opt. Express*, vol. 24, pp. 1206, 2016.
8. N. Alberto, C. Tavares, M.F. Domingues, S.F.H. Correia, C. Marques, P. Antunes, J.L. Pinto, R.A.S. Ferreira, P.S. André, "Relative humidity sensing using micro-cavities produced by the catastrophic fuse effect," *Opt. Quantum Electron.*, vol. 48, pp. 216, 2016.
9. N.T. Shelke, D.J. Late, "Hydrothermal growth of MoSe2 nanoflowers for photo- and humidity sensor applications," *Sensors Actuators A. Phys.*, vol. 295, pp. 160–168, 2019.
10. A. Urrutia, J. Goicoechea, A.L. Ricchiuti, D. Barrera, S. Sales, F.J. Arregui, "Simultaneous measurement of humidity and temperature based on a partially coated optical fiber long period grating," *Sensors Actuators B Chem.*, vol. 227, pp. 135–141, 2016.
11. E. owji, H. Mokhtari, F. Ostovari, B. Darazereshki, N. Shakiba, "2D materials coated on etched optical fibers as humidity sensors," *Scientific Reports.*, vol. 11(1), pp. 1-10, 2021.
12. W. Wei, J. Nong, G. Zhang, L.Tang, X. Jiang, N. Chen, S. Luo, G. Lan Y. Zhu, "Graphene-based long-period fiber grating surface plasmon resonance sensor for high-sensitivity gas sensing," *Sensors*, vol. 17, pp. 2, 2016.
13. Y. Huang, W. Zhu, Z. Li, G. Chen, L. Chen, J. Zhou, H. Lin, J. Guan, W. Fang, X. Liu, "High-performance fibre-optic humidity sensor based on a side-polished fibre wavelength selectively coupled with graphene oxidefilm," *Sensors Actuators B Chem.*, vol. 255, pp. 57-69, 2018.
14. R. Gao, D. Lu, J. Cheng, Y. Jiang, L. Jiang, Z. Qi, "Humidity sensor based on power leakage at resonance wavelengths of a hollow core fiber coated with reduced graphene oxide," *Sensors Actuators B Chem.*, vol. 222, pp. 618–624, 2016.
15. H. T. Su, M. J. Tsai, G. F. Chang, C.H. Hung, H. Cheng, "Solid-state sensing tip for zinc ion with double parallel optical fibers embedded in fluorescent hydrogel," *Organic Electronics*, vol. 26, pp. 429-438, 2015.
16. K. Han, S. Kim, I. Lee, J. Kim, J. H. Kim, S. Hong, B. Cho, W. Hwang, "Compliment graphene oxide coating on silk fiber surface via Electrostatic Force for Capacitive Humidity Sensor applications," *Sensors*, vol. 17, pp. 407, 2017.

17. F. Ostovari; MK. Moravvej-Farshi, “Photodetectors with zigzag andarmchair graphene nanoribbon channels and asymmetric source and drain contacts: detectors for visible and solar blind applications,” *Journal of Applied Physics*, vol. 120(14), pp. 144505, 2016.
18. Y. D. Chiu, C.-W. Wu, C. C. Chiang, “Fiber bragg grating sensor with graphene oxide coating for humidity sensing,” *Sensors*, vol. 17, pp. 2129, 2017.
19. X. Liu, X. Chen, J. Yi, Z. Luo, H. Nan, H. Guo, Z. Ni, Y. Ding, S. Dai, X. Wang, “Organic charge-transfer interface enhanced graphene hybrid phototransistors,” *Organic Electronics*, vol. 64, pp. 22-26, 2019.
20. F. Ostovari, M. Hsanpoori, M. Abbasnejad, M. A. Salehi, “DFT calculations of graphene monolayer in presence of Fe dopant and vacancy,” *Physica B: Condensed Matter*, vol. 541, pp. 6-13, 2018.
21. M. joghataei, F. Ostovari, S. Atabakhsh, N. Tobeiha, “Heterogeneous ice nucleation by graphene nanoparticles,” *Scientific Reports*, vol. 10 (1), pp. 1-9, 2020.
22. M. Ghaseminejad, L. Gholamzadeh, F. Ostovari, “Investigation of X-ray attenuation property of modification PbO with graphene in epoxy polymer,” *Materials Research Express*, vol. 8 (3), pp. 035008, 2021.
23. Z. Wang, S. Gao, T. Fei, S. Liu, and T. Zhang, “Construction of ZnO/SnO2 heterostructure on reduced graphene oxide for enhanced nitrogen dioxide sensitive performances at room temperature,” *ACS Sens.*, vol. 4(8), pp. 2048–2057, 2019.
24. A. Nag, A. Mitra, S.C. Mukhopadhyay, “Graphene and its sensor-based applications: A review,” *Sensors Actuators A Phys.*, vol. 270, pp. 177– 194, 2018.
25. P.K. Roy, G. Haider, T.C. Chou, K.H. Chen, L.C. Chen, Y.F. Chen, and C.T. Liang, “Ultrasensitive gas sensors based on vertical graphene nanowalls/SiC/Si heterostructure,” *ACS Sens.*, vol. 4(2), pp. 406–412, 2019.
26. H.F. Zhang, B. Y. Ning, T.C. Weng, D.P. Wu, X.J. Ning, “What retards the response of graphene based gaseous sensor,” *Sensors and Actuators A: Physical*, vol. 295, pp. 188-192, 2019.
27. S. Asgari, N. Geranpayeh, “Tunable mid-infrared refractive inex sensor composed of assymetric double graphene layer,” *IEEE sensors Journal*, vol. 19(14), pp. 18758143, 2019.
28. M. Ahmadian, K. Jafari, “A graphene based wide band MEMS accelerometer sensor dependent on wavelenght modulation,” *IEEE sensors Journal*, vol. 19(15), pp. 18830644, 2019.
29. S. Pei, H.M. Cheng, “The reduction of graphene oxide,” *Carbon*, vol. 50, pp. 3210–3228, 2012.
30. M. Hernaez, C.R. Zamarreño, S. Melendi-Espina, L.R. Bird, A.G. Mayes, F.J. Arregui, “Optical fibre sensors using graphene-based materials: A review,” *Sensors*, vol. 17, pp. 1–24, 2017.
31. M. Matsumoto, Y. Saito, C. Park, T. Fukushima, T. Aida, “Ultrahigh- throughput exfoliation of graphite into pristine ‘single-layer’ graphene using microwaves and molecularly enginered ionic liquids,” *Nat. Chem.*, vol. 7, pp. 730–736, 2015.
32. O.C. Compton, S.T. Nguyen, “Graphene Oxide, Highly reduced graphene oxide, and graphene: versatile building blocks for carbon-based materials,” *Small*, vol. 6, pp. 711–723, 2010.

33. F. Ostovari, Y. Abdi, S. Darbari, F. Ghasemi, “Effects of electromechanical resonance on photocatalytic reduction of the free- hanging graphene oxide sheets,” *Journal of nanoparticle research*, vol. 15(4), pp. 1551, 2013.
34. W. Hummers, R. Offeman, “Preparation of graphitic oxide,” *J. Am. Chem. Soc.*, pp. 1339, 1958.
35. H.A. Rivera Tito, A. Habermehl, C. Müller, S. Beck, C. Romero Nieto, G. Hernández Sosa, M.E. Quintana Caceda, “Electrical and optical properties of reduced graphene oxide thin film deposited onto polyethylene terephthalate by spin coating technique,” *Appl. Opt.*, vol. 56, pp. 7774, 2017.
36. A. Gholampour, M. Valizadeh Kiamahalleh, D.N.H. Tran, T. Ozbakkaloglu, D. Losic, “From graphene oxide to reduced graphene Oxide: impact on the physiochemical and mechanical properties of graphene–cement composites,” *ACS Appl. Mater. Interfaces*, vol. 9, pp. 43275–43286, 2017.
37. I.K. Moon, J. Lee, R.S. Ruoff, H. Lee, “Reduced graphene oxide by chemical graphitization,” *Nat. Commun.*, vol. 1, pp. 73, 2010.
38. E. Nossol, A.B.S. Nossol, S.X. Guo, J. Zhang, X.Y. Fang, A.J.G. Zarbin, A.M. Bond, “Synthesis, characterization and morphology of reduced graphene oxide–metal–TCNQ nanocomposites,” *J. Mater. Chem. C*, vol 2, pp. 870–878, 2014.
39. C. Zhu, S. Guo, Y. Fang, S. Dong, “Reducing sugar: new functional molecules for the green synthesis of graphene nanosheets,” *ACS Nano*, vol. 4, pp. 2429–2437, 2010.
40. E. Rommozzi, M. Zannotti, R. Giovannetti, C. D’Amato, S. Ferraro, M. Minicucci, R. Gunnella, A. Di Cicco, “Reduced graphene Oxide/TiO2 nanocomposite: from synthesis to characterization for efficient visible light photocatalytic applications,” *Catalysts*, vol. 8, pp. 598, 2018.
41. M. Todica, T. Stefan, S. Simon, I. Balasz, L. Daraban, “UV-Vis and XRD investigation of graphite-doped poly(acrylic) acid membranes,” *TURKISH J. Phys.*, vol. 38, pp. 261–267, 2014.
42. G. Rajan, “Optical Fiber Humidity Sensors,” in *Optical fiber sensors: advanced techniques and applications (Devices, Circuits, and Systems)*, 1st ed., CRC Pres, 2015, ch. 15, pp. 413-455.
43. G. Naik, S. Krishnaswamy, “Room-temperature humidity sensing using graphene oxide thin films,” *Graphene*, vol. 05, pp. 1-13, 2016.
44. G. Y. Chen, “A review of microfiber and nanofiber based optical sensors,” *Open Opt. J.*, vol. 7, pp. 32–57, 2013.

Figures

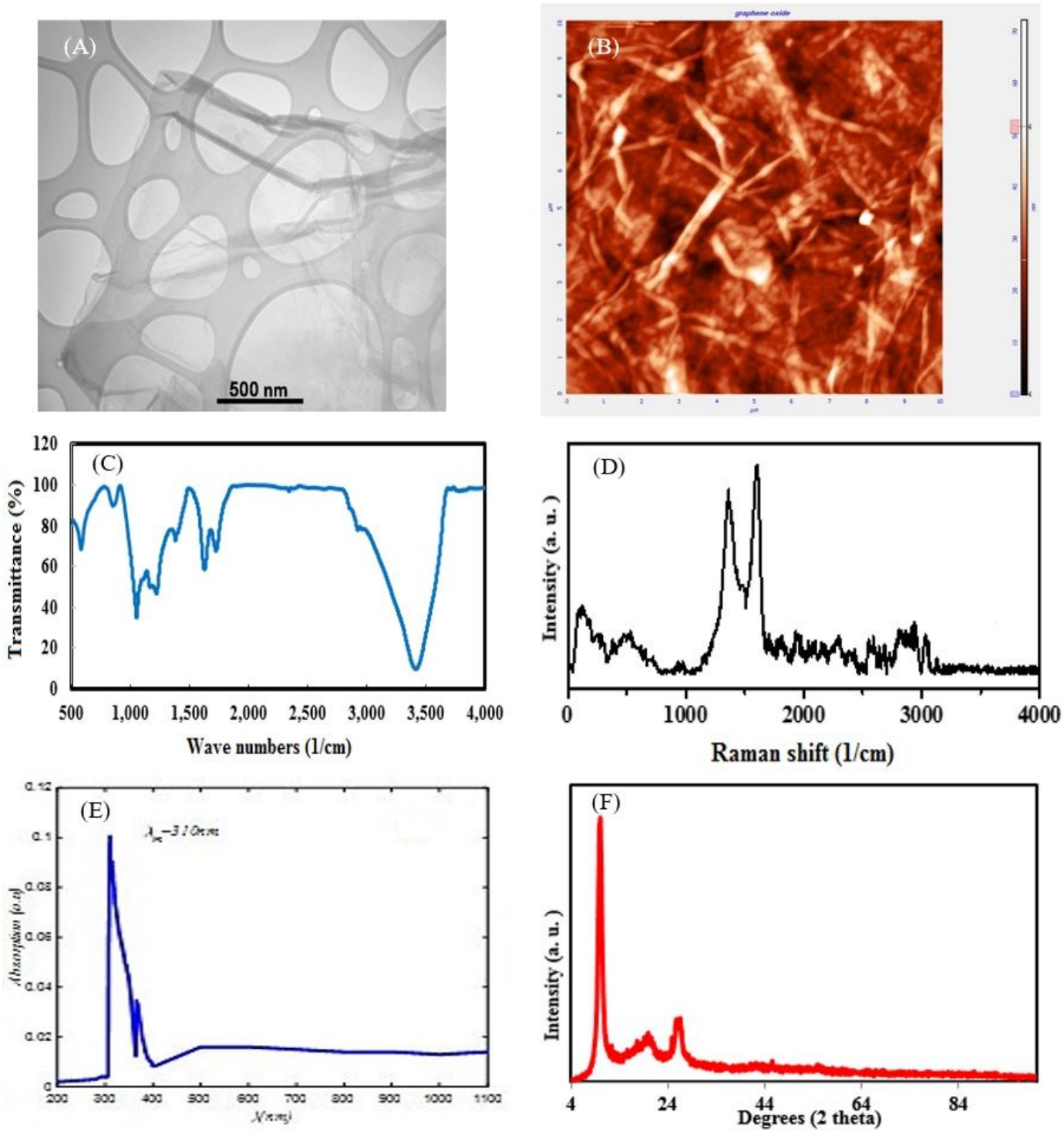

Figure 1

A) TEM, B) AFM, C) FTIR, D) Raman, E) UV-Visible and F) XRD analysis of GO.

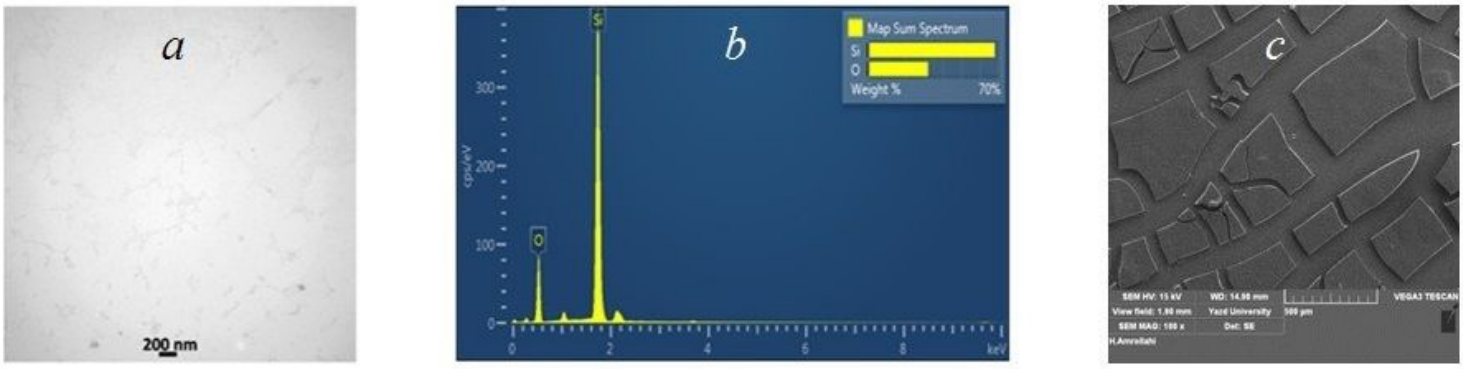

Figure 2

A) TEM image, B) EDX spectrum of Sg and C) SEM image of GSg

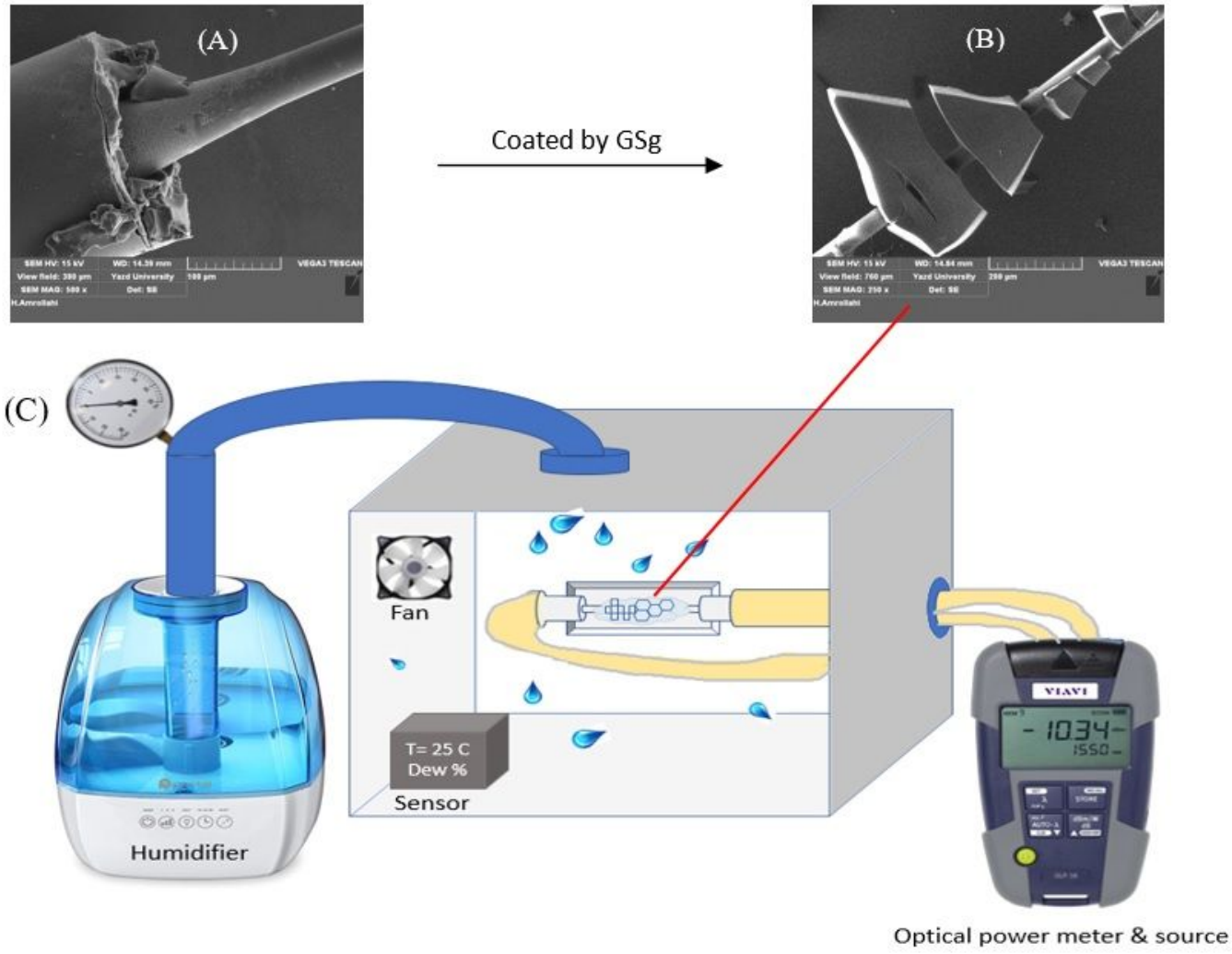

Figure 3

A) SEM image of the etched SMF after 60 minutes of corrosion with HF, B) SEM image of the etched SMF coated with GSg, C) set up tools to analyze humidity sensing.

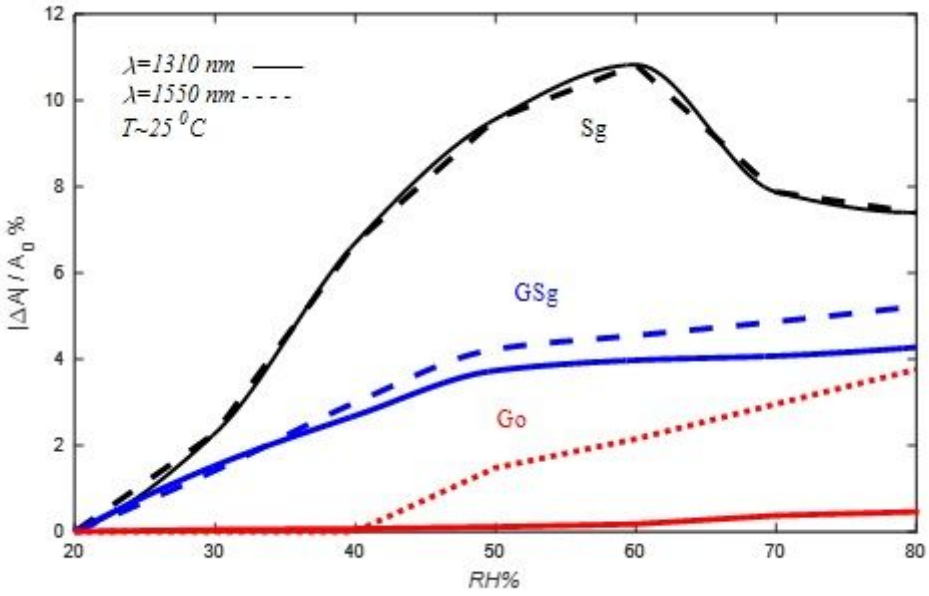

Figure 4

RDA as a function of RH at both wavelengths for GO, Sg and GSg.

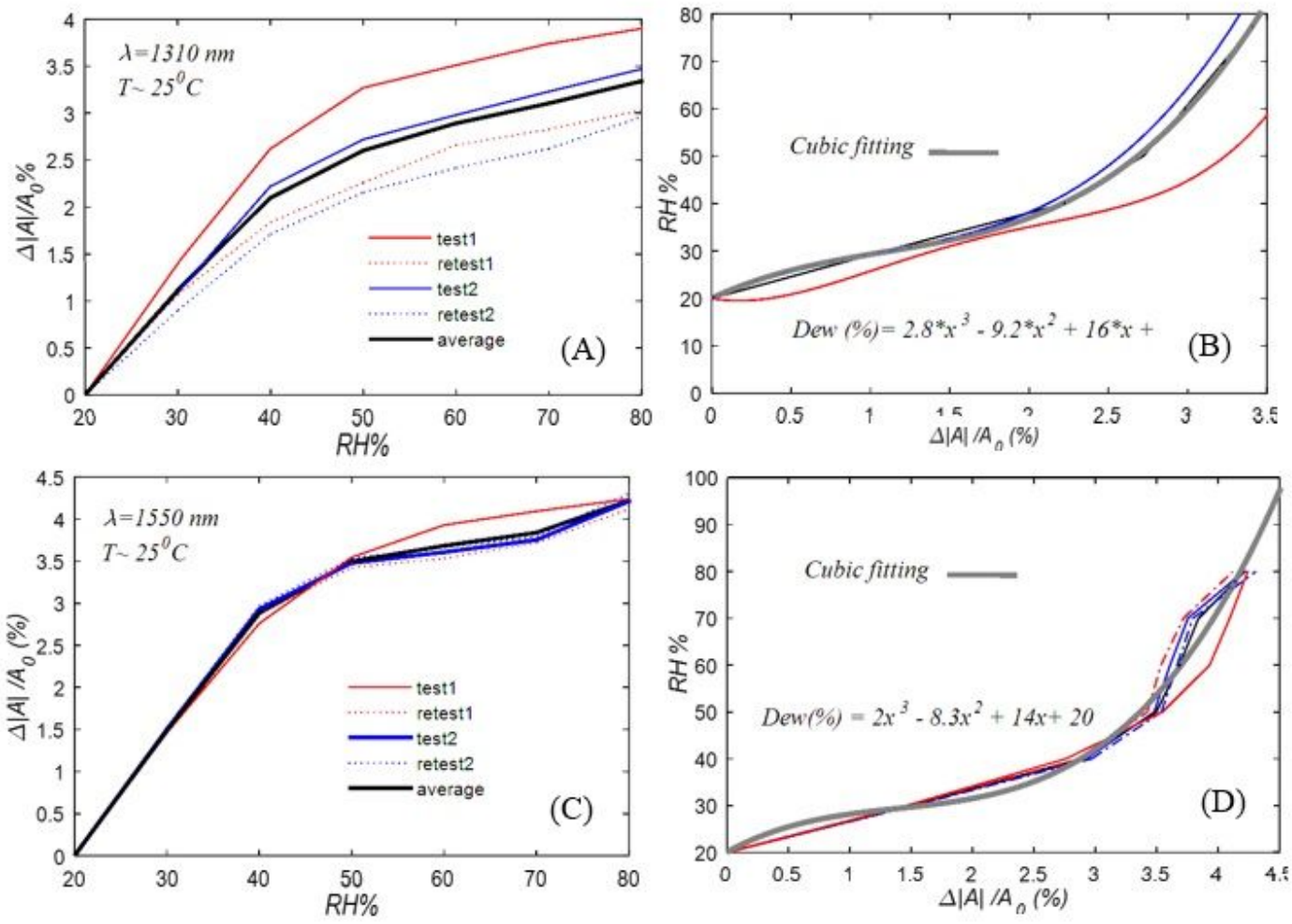

Figure 5

Repeatability of RDA as a function of RH for SGg at (A) 1310-nm and (C) 1550-nm wavelengths; Reverse and fitting curves to calculate the RH values at (B) 1310 nm and (D) 1550 nm wavelengths (Dash-line curves are the rapid retest of the solid-line curves).

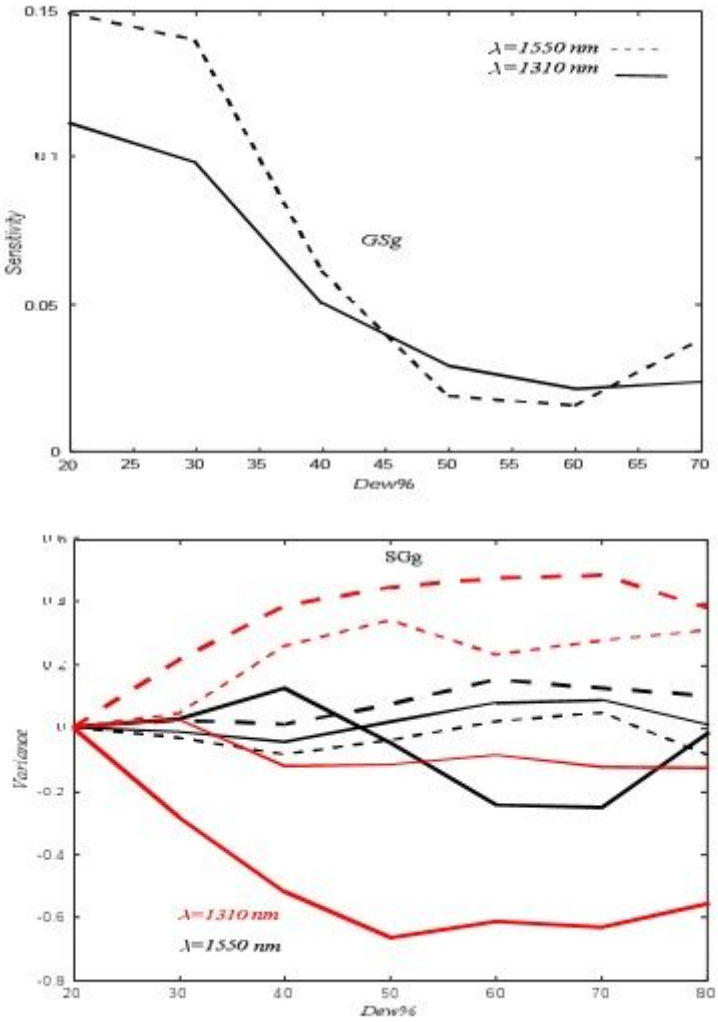

Figure 6

A) Sensitivity of the etched fibers coated with SCg to humidity at the wavelength of 1310 nm (The solid line curves) and 1550 nm (The dash-line curves), B) Variance as a function of RH from the average values of SGg at the 1310-nm and 1550-nm wavelengths.